

Effect of piping systems on surge in centrifugal compressors[†]

Hideaki Tamaki*

*Turbomachinery and Engine Technology Department, Products Development Center, IHI Corporation 1,
Shin-nakahara-cho, Isogo-ku, Yokohama 235-8501, Japan*

(Manuscript Received April 16, 2008; Revised June 25, 2008; Accepted July 23, 2008)

Abstract

There is a possibility that the exchange of the piping system may change the surge characteristic of a compressor. The piping system of a plant is not always the same as that of a test site. Then it is important to evaluate the effect of piping systems on surge characteristics in centrifugal compressors. Several turbochargers combined with different piping systems were tested. The lumped parameter model which was simplified to be solved easily was applied for the prediction of surge point. Surge lines were calculated with the linearized lumped parameter model. The difference between the test and calculated results was within 10 %. Trajectory of surge cycle was also examined by solving the lumped parameter model. Mild surge and deep surge were successfully predicted. This study confirmed that the lumped parameter model was a very useful tool to predict the effect of piping systems on surge characteristics in centrifugal compressors, even though that was a simple model.

Keywords: Centrifugal compressor; Performance; Surge; Lumped parameter model

1. Introduction

Surge is a system oscillation caused by the interaction of the compressor and piping system characteristics. Hence, there is a possibility that the application of different piping system to the specific compressor may change the characteristics of surge. When the piping system of a plant is not the same as that of a test stand, different surge characteristics might be encountered. Surge characteristics of the compressors for the automotive turbochargers, in particular, tend to be influenced by the difference of the piping systems, because of their small sizes. The compressors for automotive turbochargers are often used at the left side of the peak pressure points on their performance map, total to total pressure ratio versus flow rate, because of the requirement of the wide operating range to deal with the engine operation from the idling to the rated speed. The piping systems are con-

sidered to have a strong influence on the stability of the compressor operation at the left side of the peak pressure point. During the development of a compressor, it is a concern that the applications of the several different piping systems to the experiments bring about the various surge characteristics that depend on the piping system and the characteristics of surge become obscure. Hence it is important to predict the effect of the piping systems on the surge characteristics to the design of the compressor and plan the experiment accordingly. Several centrifugal compressors for turbochargers combined with the different piping systems were tested and the changes of surge characteristics, surge lines which connect surge points on the performance map, were investigated. Then the lumped parameter model [1] was applied for the tested compression systems and its effectiveness for the prediction of surge line was examined.

2. Experimental apparatus

The diameters of the tested compressor impellers

[†] This paper was presented at the 9th Asian International Conference on Fluid Machinery (AICFM9), Jeju, Korea, October 16-19, 2007.

*Corresponding author. Tel.: +81 45 759 2870, Fax.: +81 45 759 2205

E-mail address: hideaki_tamaki@ihi.co.jp

© KSME & Springer 2008

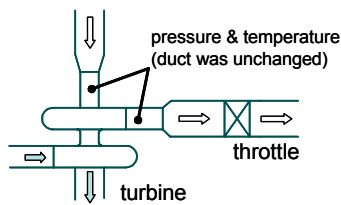
are listed in Table 1. All the compressors are for automotive turbochargers. Fig. 1 shows the schematics of the compression systems and the dimensions of the piping systems applied in this study. The dimensions of H2 are non-dimensionalized by those of H1. The dimensions of H4, H5 and H6 are non-dimensionalized by those of H3. The dimensions of H8 is non-dimensionalized by those of H7. Table 2 shows the combinations of the compressors and the piping systems which were tested.

The ducts in the piping systems are considered to be a pipe whose area is constant and equal to the impeller inlet eye area and their lengths are defined by,

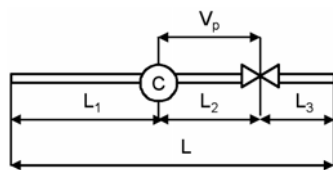
$$\frac{L_i}{A_c} = \int_i \frac{dx}{A(x)} \quad (i=1 \text{ to } 3)$$

Table 1. Tested Compressor impeller diameter.

Compressor	A	B	C	D	E	F
D ₂ (mm)	92	52.5	58	48	50	82



(a)



Piping System	L ₁	L ₂	L ₃	V _p	L
H1	0.38L	0.20L	0.42L	1.00	1.00
H2	0.25L	0.08L	0.20L	9.14	0.53L

Piping System	L ₁	L ₂	L ₃	V _p	L
H3	0.25L	0.09L	0.67L	1.00	1.00
H4	0.16L	0.12L	0.03L	42.00	0.31
H5	0.14L	0.17L	0.46L	1.80	0.78
H6	0.25L	0.27L	0.13L	1.54	0.66

Piping System	L ₁	L ₂	L ₃	V _p	L
H7	0.38L	0.28L	0.34L	1.00	1.00
H8	0.07L	0.24L	0.23L	1.69	0.54L

(b)

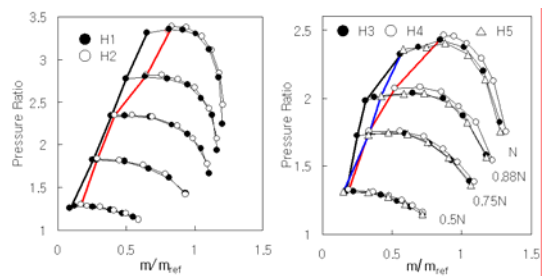
Fig. 1. (a) Schematic of compression systems (b) Tested piping system dimensions.

where A_c is the impeller inlet eye area. x is a length of the duct and A(x) is a sectional area of the duct. i = 1, 2 and 3 correspond to the compressor inlet, the region from the compressor outlet to the throttle, and downstream of the throttle respectively. V_p is the plenum volume downstream of the compressor which is defined by the volume of the duct from the compressor outlet to the throttle valve.

3. Results and discussion

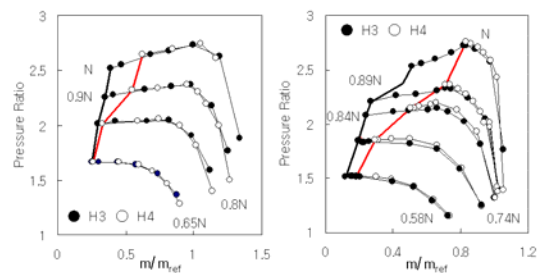
3.1 Test results

The measured performance maps of total to total pressure ratio versus flow rate, including data for the different piping systems, are shown in Fig. 2. It is speculated that the change of the piping system was



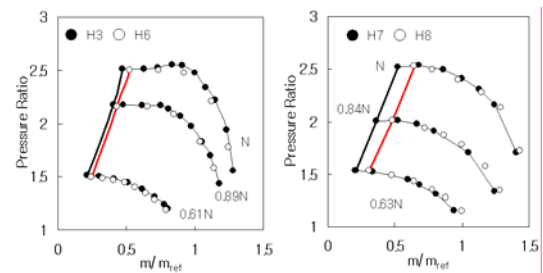
(a) Compressor A

(b) Compressor B



(c) Compressor C

(d) Compressor D



(e) Compressor E

(f) Compressor F

Fig. 2. Compressor performance map.

responsible for the different surge lines. An important non-dimensional parameter describing the dynamics of the compression systems is

$$B = \frac{U}{2a_p} \sqrt{\frac{V_p}{A_c L}}$$

where U is the impeller tip speed, a_p is the speed of sound calculated with the compressor exit total temperature at the maximum efficiency point for each rotational speed. B for the tested compression systems is included in Table 2. The compression system tends to exhibit unsteadiness as the value of B increases [2]. Higher rotational speed makes B larger. Hence the difference of the surge line became greater, as the rotational speed increases. The largest difference between a small value of B and a large value of B among the tested compressors is the case of compressor D. The change of surge line from the small B to large B was the largest for all the rotational speeds, accordingly.

Table 2. Combination of compressor and piping system and value of B for minimum and maximum rotational speed.

Compressor	Piping System	B Parameter	
		N_{min}	N
A	H1	0.15	0.31
	H2	0.61	1.27
B	H3	0.14	0.24
	H4	1.59	2.82
	H5	0.21	0.37
C	H3	0.13	0.18
	H4	1.55	2.15
D	H3	0.18	0.28
	H4	2.10	3.25
E	H3	0.27	0.41
	H6	0.41	0.63
F	H7	0.35	0.50
	H8	1.67	2.42

(N_{min} is minimum rotational speed for each test condition.)

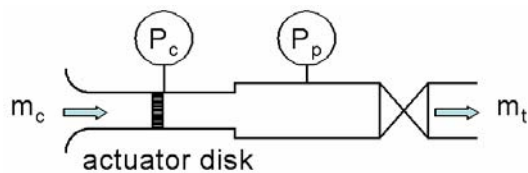


Fig. 3. Model of compression system.

3.2 Prediction of surge line

The compression system discussed is shown in Fig. 3. The system includes an inlet duct, a compressor, an outlet duct, a plenum, and a throttle. The lumped parameter compression model will be used to predict the surge line. The major assumptions are:

- (1) One-dimensional incompressible flow in the duct.
- (2) Isentropic expansion or compression in the plenum.
- (3) Negligible velocity in the plenum.
- (4) Compressor was modeled as an actuator disk.
- (5) Throttle duct length is short.

The equations of the conservation of momentum in the duct and the conservation of mass flow in the plenum can be written as:

$$\frac{L}{A_c} \frac{dm_c}{dt} = P_c - P_p \tag{1}$$

$$\frac{d(\rho_p V_p)}{dt} = m_c - m_t \tag{2}$$

For the simplification, the assumption that the compression system is driven by the pressure difference between the compressor exit and the plenum is applied to Eq. (1). The process in the plenum is assumed to be isentropic. The relationship between pressure and density is written as

$$\frac{dP_p}{P_p} = \gamma \frac{d\rho_p}{\rho_p}$$

where γ is specific heat ratio. Using this equation, Eq. (2) is modified

$$\frac{dP_p}{dt} = \frac{a_p^2}{V_p} (m_c - m_t) \tag{2a}$$

Applying the small perturbation analysis [3] to the equations above, Eq. (3) and (4) can be derived.

$$\frac{d\delta m_c}{dt} = \frac{A_c}{L} \left(\frac{d\bar{P}_c}{dm_c} \delta m_c - \delta P_p \right) \tag{3}$$

$$\frac{d\delta P_p}{dt} = \frac{a_p^2}{V_p} (\delta m_c - \delta m_t) \tag{4}$$

where ‘-’ and ‘ δ ’ show the steady and small perturbation.

tion term respectively.

The pressure drop at the throttle, ΔP_t , is

$$\Delta P_t = P_p - P_a$$

Then the relationship between δm_t and δP_p is given by

$$\delta P_p = \left(\frac{d\Delta P_t}{dm_t} \right) \delta m_t \tag{5}$$

The slope of the pressure drop at the valve can be approximated by Eq. (6).

$$\frac{d\Delta P_t}{dm_t} = \frac{\bar{P}_c - P_a}{m_c} \tag{6}$$

The performance curve, relationship between total to total pressure ratio and mass flow rate at a specific rotational speed, was model by a 2nd order polynomial. As the important part on the performance map for the prediction of surge is the lower flow region, it was considered that a 2nd order polynomial had enough accuracy to approximate the lower flow region on the performance curve.

Using Eq. (5) and (6), Eq. (3) and (4) are modified

$$\frac{d}{dt} \begin{pmatrix} \delta m_c \\ \delta P_p \end{pmatrix} = \begin{pmatrix} b_{11} & b_{12} \\ b_{21} & b_{22} \end{pmatrix} \begin{pmatrix} \delta m_c \\ \delta P_p \end{pmatrix} = B \begin{pmatrix} \delta m_c \\ \delta P_p \end{pmatrix} \tag{7}$$

$$b_{11} = \frac{A_c}{L} \frac{d\bar{P}_c}{dm_c} \quad b_{12} = -\frac{A_c}{L}$$

$$b_{21} = \frac{a_p^2}{V_p} \quad b_{22} = -\frac{a_p^2}{V_p} \frac{m_c}{P_c - P_a}$$

Instability of the compression system can be predicted by solving the eigenvalues of matrix B. When one or more real parts of the eigenvalues are larger than zero, instability (surge) will occur in the compression system. The eigenvalues can be obtained by solving the quadratic equation whose coefficients are defined by the performance curve.

The comparisons of the predicted results and the tested results are shown in Fig. 4. It is found that the effect of the piping systems on surge line is properly reflected by the calculation. Fig. 5 also shows the comparison of the predicted results and the tested results. The prediction results are within $\pm 5\%$ except

compressor C with H4 and compressor D with H3 and most of the predicted results are within $\pm 10\%$. As the performance curves of compressor C and D are

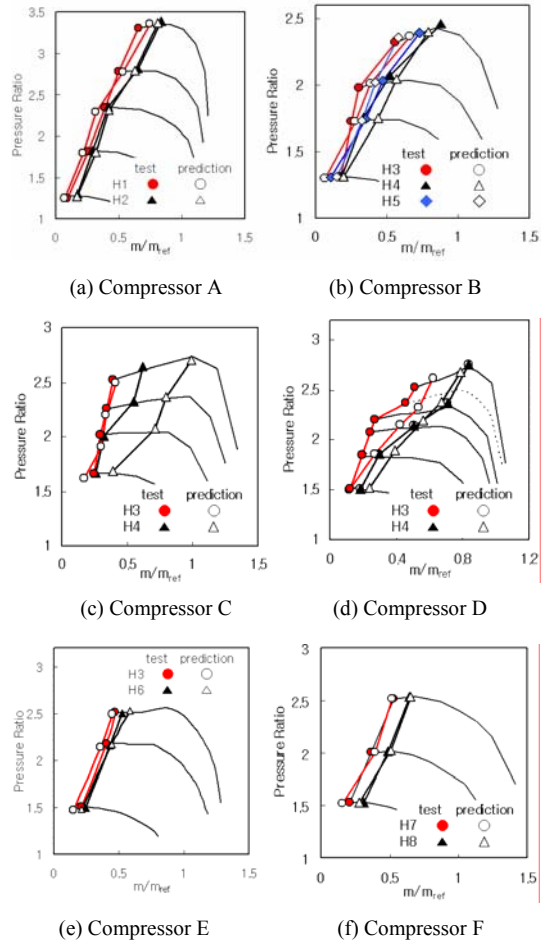


Fig. 4. Comparisons of predicted and tested surge line.

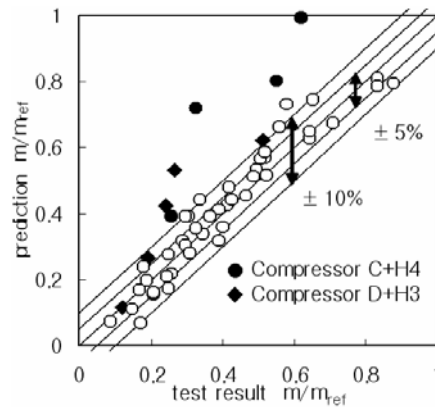


Fig. 5. Comparisons of predicted and tested result.

almost linear at the lower flow region, the 2nd order polynomial approximation of the compressor performance might be inadequate in this region. However it is thought that this prediction method is useful enough to estimate the change of surge line by the change of the piping system, using the performance map of an existing compressor whose specification is similar to the compressor which a designer wants to test.

3.3 Simulation of surge transients

Compressors for turbochargers often encounter mild surge before (deep) surge. Fig. 6 shows an example of the static pressure fluctuations of Compressor D. These data were obtained by closing the throttle from mild surge condition to surge rapidly. The oscillation with smaller amplitude and higher frequency than surge was observed before surge. As for the temperature (data was not shown), the compressor inlet temperature was almost constant before surge, even if the pressure oscillation was observed. Then the compressor inlet temperature started to increase rapidly, after the operation of the compressor went into surge. The oscillation before surge was considered as mild surge which does not accompany the reverse flow in the compression system. Similar oscillations, mild surge, appeared at Compressor A with H1, Compressor B with H3 and Compressor D with H3. Fig. 7 shows the compressor maps of Compressor D with mild surge lines.

In order to investigate the effect of the piping systems on the pressure fluctuation, the system of equations was integrated numerically.

The equations of the conservation of momentum in the duct and the conservation mass flow in the plenum are

$$\frac{L}{A_c} \frac{dm_c}{dt} = P_c - P_p \tag{1}$$

$$\frac{dP_p}{dt} = \frac{a_p^2}{V_p} (m_c - m_t) \tag{2a}$$

The relation between the instantaneous and steady state compressor pressure rise is written as

$$\frac{dP_c}{dt} = \frac{1}{\tau} (\bar{P}_c - P_c) \tag{8}$$

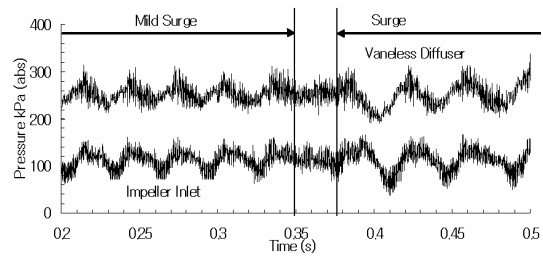


Fig. 6. Pressure fluctuation from mild surge to surge (Compressor D at rotational speed of N).

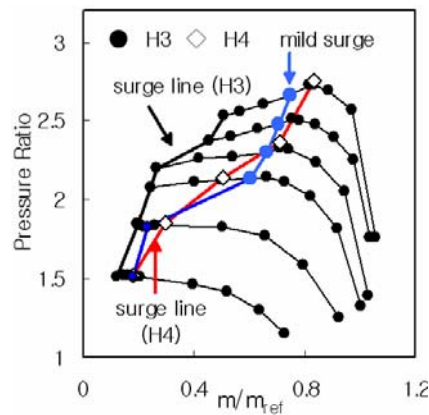


Fig. 7. Performance of compressor D with mild surge line.

where τ refers to the compressor through-flow time and is assumed to be

$$\tau = \frac{L_t}{C}$$

L_t is the meridional length of the impeller and diffuser. C is the average meridional velocity.

The flow through the throttle is related to the pressure drop at the throttle as given by

$$\Delta P_t = P_p - P_a = \frac{1}{2} \xi \frac{m_t^2}{\rho_p A_t^2} \tag{9}$$

Eq. (9) is rearranged and it becomes

$$m_t = A_t \sqrt{\frac{2\rho_p}{\xi} (P_p - P_a)} \tag{9a}$$

$$\xi = 2\rho_p A_t^2 \frac{(P_p - P_a)}{m_t^2} \tag{9b}$$

Eq. (1), (2a), (8) and (9a) were solved.

The throttle was set at the peak pressure point on the performance map, and then the throttle was closed to the specific point on the performance curve in a short time. During this period, the pressure in plenum was assumed to be constant, the same as the peak pressure on the performance curve, thus ξ was time dependent. After this period, ξ was assumed to be constant. The oscillation was calculated during and after the above operation of the throttle. The pressure oscillation in the compressor depends on the performance curve. As the compressor operating point during the oscillation would move from choke to the left side of surge, an accurate performance curve is desirable on the whole flow range and the performance curve on the left side of surge should be assumed. Fig. 8 shows the formulation of the performance curve used in the calculation. The 4th order Runge-Kutta method was applied to the integration.

Fig. 9 is the calculated result for the compression system of Compressor D at the highest rotational speed. Compressor D with H3 shows oscillations with and without reverse flow depending on the operating point. However the oscillation without the reverse flow was not obtained for Compressor D with H4.

Eqs. (1) and (2a) are rewritten by the introduction of the nondimensional mass flow, pressure and time [4].

$$\frac{d\tilde{m}_c}{d\tilde{t}} = B(\tilde{P}_c - \tilde{P}_p) \tag{1a}$$

$$\frac{d\tilde{P}_p}{d\tilde{t}} = \frac{1}{B^2}(\tilde{m}_c - \tilde{m}_t) \tag{2b}$$

where mass flow is divided by ρUA , pressure is divided by $\rho U^2/2$ and time is divided by $1/\omega$ ($\omega = a_p [A/$

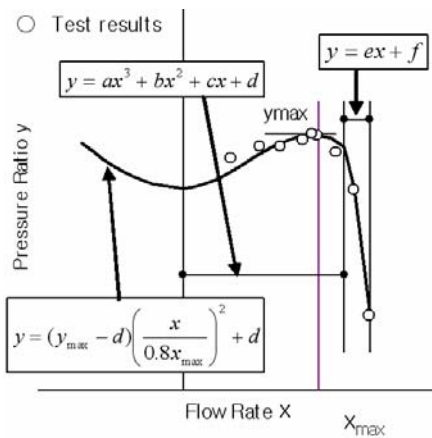


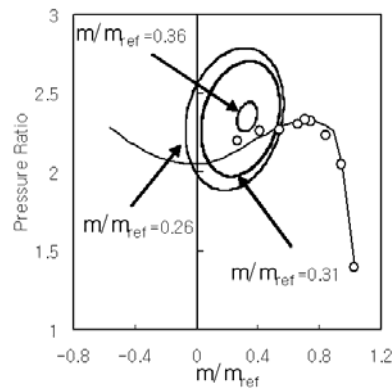
Fig. 8. Performance curve applied for calculation.

$(V_p L)]^{0.5}$).

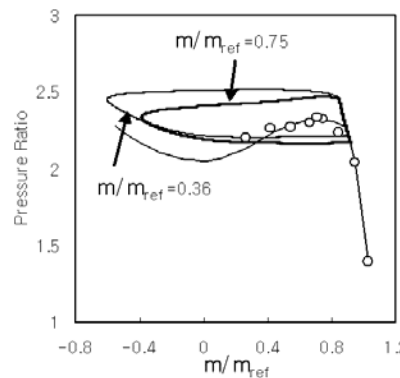
The mass flow fluctuation is proportional to B and the pressure fluctuation is inversely proportional to B². As B of H3 is small, the change of the flow rate is small and that of the pressure is large. As B of H4 is about 11 times larger than that of H3, then the change of the flow rate is large and that of the pressure is small. Hence the trajectory of the oscillation of H3 became a closed curve like an ellipse with the major axis parallel to the axis of the pressure ratio and that of H4 became a closed curve like a rectangle whose length was parallel to the axis of the flow rate. This result suggests that the shape of the trajectory could be used to estimate whether mild surge can be measured or not in the piping system which a designer chooses.

4. Conclusion

- (1) The test results showed that the changes in the duct length or plenum volume in the compres



(a) Surge cycle of compressor D with H3



(b) Surge cycle of compressor D with H4

Fig. 9. Calculated surge cycle of Compressor D.

- sion system changed the surge line.
- (2) The simplified lumped parameter model with small perturbation analysis was applied for the prediction of surge line. The effect of the piping systems on surge line was properly reflected by the calculation. The difference between the test and calculated results was within 10 %.
 - (3) The transient simulation was done by integrating the lumped parameter model. Mild surge, or oscillation without reverse flow, was obtained for a small value of B. The shape of the trajectory obtained by the lumped parameter model is useful to estimate whether mild surge can be measured or not by the designed piping system.

Acknowledgments

The author wants to thank Dr. Dai Ji of Institute of Engineering Thermophysics, Chinese Academy of Science for his support to construct the analytical model.

Nomenclature

Ac	: Reference area
At	: Aarea upstream of throttle
a_p	: Sonic speed in plenum
D_2	: Impeller diameter (mm)
L	: Length (m)
m	: Mass flow rate (kg/s)
m_{ref}	: Reference mass flow rate (kg/s)
N	: Reference rotational speed (rpm)

P	: Pressure
ΔP_t	: Total pressure drop at throttle
t	: Time (s)
U	: Impeller tip speed (m/s)
V_p	: Volume of plenum (m^3)

Greeks

τ	: Time constant
ξ	: Pressure loss coefficient at throttle
ρ	: Density

Subscripts

a	: Atmospheric condition
c	: Compressor exit
p	: Plenum
t	: Downstream of throttle

References

- [1] E. M. Greitzer, The stability of pump systems the 1980 freeman scholar lecture, *Trans., ASME Journal of Engineering for Power*, 113 (1981) 193-242.
- [2] D. A. Fink, N. A. Cumpsty and E. M. Greitzer, Surge dynamics in a free-spool centrifugal compressor system, *Trans., ASME Journal of Engineering for Power*, 114 (1992) 321-332.
- [3] C. Gu, S. Wen, M. Zang and D. Ji, A study of calculational model for predicting surge line in a centrifugal compression system with cooler and condenser, ASME Papers, 97-AA-109, (1997).
- [4] R. C. Pampreen, compressor surge and stall, Concept ETI, Inc., USA, (1993).